Available online at www.sciencedirect.com
SCIENCE DIRECT®
Applied Surface Science 231–232 (2004) 131–135
applied surface science
www.elsevier.com/locate/apsusc

Desorption/ionization of molecular nanoclusters: SIMS versus MALDI

A. Delcorte[a,*], S. Hermans[b], M. Devillers[b], N. Lourette[c], F. Aubriet[c], J.-F. Muller[c], P. Bertrand[a]

[a]*Unité de Physico-Chimie et de Physique des Matériaux, Université Catholique de Louvain, Croix du Sud 1, Louvain-la-Neuve B-1348, Belgium*
[b]*Unité de Chimie des Matériaux Inorganiques et Organiques, Université Catholique de Louvain, Place L. Pasteur 1, Louvain-la-Neuve B-1348, Belgium*
[c]*Laboratoire de Spectrométrie de Masse et de Chimie Laser, Université de Metz, Boulevard Arago 1, F-57078, Metz, France*

Available online 25 May 2004

Abstract

Molecular nanoclusters, consisting of a core with a few metal atoms surrounded by a protective layer of organic ligands and potentially useful for heterogeneous catalysis applications, have been analyzed using energetic beam (particle/laser)-induced mass spectrometry. The results are mainly illustrated by the study of the molecular precursor $[Ru_5C(CO)_{14}Pt(C_8H_{12})]$ cast on a silicon substrate from dilute acetone or acetonitrile solutions. In both ToF-SIMS and MALDI-ToF, the molecular ion does not dominate the high-mass range of the mass spectrum. Instead, the dominant peak series correspond to the molecular cluster having lost its hydrocarbon residue and/or a number of CO ligands, with some specifics for each desorption/ionization method. The processes leading to the constitution of the mass spectrum for such compounds (surface fragmentation, unimolecular dissociation) are investigated through the comparison of the SIMS and MALDI data. Perspectives concerning the usefulness of these two techniques for the analysis of supported nanoclusters (real catalysts) are provided in the conclusion.

Keywords: SIMS; MALDI; Nanoclusters; Metal clusters; Catalysts; Ion emission

1. Introduction

Molecular nanoclusters receive much attention because of their promising applications as nano-building blocks in various fields including catalysis, particularly when they contain different elements in their core [1,2]. A key question concerns the preservation of these entities when they are incorporated on a catalyst support, and the way they degrade upon thermal treatment to generate the active heterometallic nanoparticles.

To our knowledge, these objects have never been studied by secondary ion mass spectrometry (SIMS) and only few reports exist concerning their characterization by laser desorption ionization (LDI) [3]. The potential advantage of such methods lies in their ability to provide a direct assessment of the chemical

* Corresponding author.
E-mail address: delcorte@pcpm.ucl.ac.be (A. Delcorte).

0169-4332/$ – see front matter © 2004 Elsevier B.V. All rights reserved.
doi:10.1016/j.apsusc.2004.03.092

reactions/structural changes experienced by the molecular nanocluster upon adsorption and further treatments on various substrates.

In this preliminary study, we investigate the mass spectrometric fingerprint of $[Ru_5C(CO)_{14}Pt(C_8H_{12})]$ nanoclusters either physisorbed on a silicon substrate (ToF-SIMS) or embedded in a non-reactive dithranol matrix (MALDI-ToF). These investigations should help us ground the analysis of more complex samples that are useful in catalytic applications.

2. Materials and methods

2.1. Samples

The nanocluster sample chosen for this study is $[Ru_5C(CO)_{14}Pt(C_8H_{12})]$. Its structure, as determined by X-ray crystallographic analysis, is shown in Fig. 1. This cluster was synthesized according to a previous report [4], by reacting the reduced dianionic $[PPN]_2[Ru_5C(CO)_{14}]$ cluster with $[Pt(C_8H_{12})Cl_2]$ in the presence of silica. The silica was believed to assist the removal of Cl^- from the platinum(II) complex, thus creating highly reactive dicationic Pt fragments adsorbed on its surface. The mixed-metal cluster was then formed by simple addition of the pentaruthenium dianion and the monometallic platinum dication. The structure of the obtained mixed species (Fig. 1) confirms this mechanism: the geometry of the starting pyramidal Ru_5C cluster is unchanged, with the square face of the pyramid capped by a $Pt(C_8H_{12})$ fragment. This Ru_5Pt cluster is stable in air, and soluble in most organic solvents, thus easy to handle. It was fully characterized by multinuclear NMR, infrared spectroscopy, elemental analysis and X-ray crystallography, before being considered for the present study.

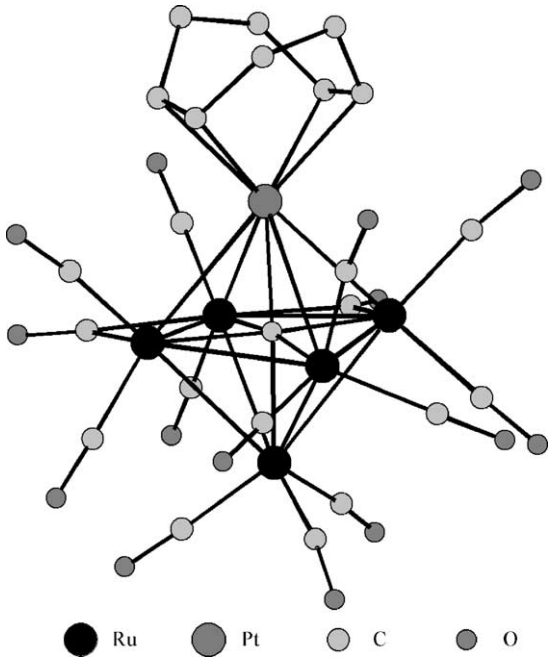

Fig. 1. Molecular structure of the cluster $[Ru_5C(CO)_{14}Pt(C_8H_{12})]$, as determined by single crystal X-ray crystallography. Hydrogen atoms on the C_8H_{12} (cyclooctadiene) ligand are omitted for clarity.

For the SIMS analyses, the nanocluster sample was dissolved in acetone (~1 mg/ml) and cast on a clean silicon wafer cut down to ~1 cm^2. For the MALDI analyses, dithranol was used as a matrix. Solutions of acetonitrile with 1 or 10 mg/ml of dithranol and an analyte/matrix weight ratio of 10^{-3} to 10^{-6} were prepared. The solutions were directly cast on the stainless steel sample holder of the MALDI instrument. It is useful to note that the same procedure was tested without success using 2,5-dihydroxybenzoic acid instead of dithranol.

2.2. Experimental setup

The secondary ion mass analyses and images were acquired in a PHI-EVANS Time-of-Flight SIMS (TRIFT 1) using a 15 keV Ga^+ beam (FEI 83-2 liquid metal ion source; ~550 pA DC current; 22 ns pulse width bunched down to ~1 ns; 5 kHz repetition rate for the mass range 0–5 kDa) [5]. The experimental setup has been described in detail elsewhere [6]. The ToF-SIMS spectra presented hereafter were obtained from the collection of the secondary ion signal in the mass range $0 < m/z < 5000$ for the 1800 s bombardment of a 180 μm × 180 μm sample area, corresponding to a fluence of 1.05×10^{12} ions/cm^2. To improve the measured intensities, the secondary ions were post-accelerated by a high voltage (7 kV) in front of the detector.

The MALDI spectra were obtained using a Bruker Reflex IV Maldi-ToF instrument (Bruker-Franzen Analytik GmbH, Bremen, Germany) equipped with a delayed extraction. Ionization was achieved by using a nitrogen laser ($\lambda = 337$ nm, pulse duration: 3 ns,

output energy: 400 μJ, repetition rate: 5 Hz). The laser diameter was around 30 μm. The laser fluence was typically kept in our experiments at 75 mJ/cm^2. The mass spectrometer was operated in the reflectron mode at a total acceleration voltage of 20 kV and a reflecting voltage of 23 kV. A delay time of 400 ns was used prior to ion extraction. The mass spectra were the result of the accumulation of 600 laser shots on different places of the same sample and were acquired in the 0–2000 Da mass range. The ion assignment was attained after external calibration performed with the cationized cluster ions emitted from a standard CrO_3 sample. The mass spectrum presented hereafter is from raw data with no baseline correction and no signal smoothing.

3. Results and discussion

The goal of this study is to obtain standard ion mass spectra of Ru–Pt nanocluster samples under keV ion and UV laser bombardment, prior to a more complete investigation of the supported clusters specifically designed for catalytic applications. In this section, we first describe the SIMS spectra (Section 3.1), then the MALDI spectra (Section 3.2). The discussion focuses on the interpretation of the specific features encountered in these mass spectra and on the differences between the results obtained with the two ionization methods.

3.1. SIMS spectra

The positive and negative mass spectra of [$Ru_5C(CO)_{14}Pt(C_8H_{12})$] are displayed in Fig. 2a and b. Instead of isolated peaks, the characteristic features in the high-mass region of the spectra are broad distributions of peaks, disseminated between 800 and 1250 Da. The molecular ion peaks, although not predominant, are present in both spectra around $m/z = 1213$ Da. Some other peak distributions are identified on the spectra of Fig. 2, namely, the series of peaks induced by the loss of a number of CO ligands, in the positive mass spectrum, and those resulting from the loss of the C_8H_{12} group and a number of CO fragments, in the negative mass spectrum.

The complexity of the mass spectra not only arises from the wide isotopic distribution of the molecular

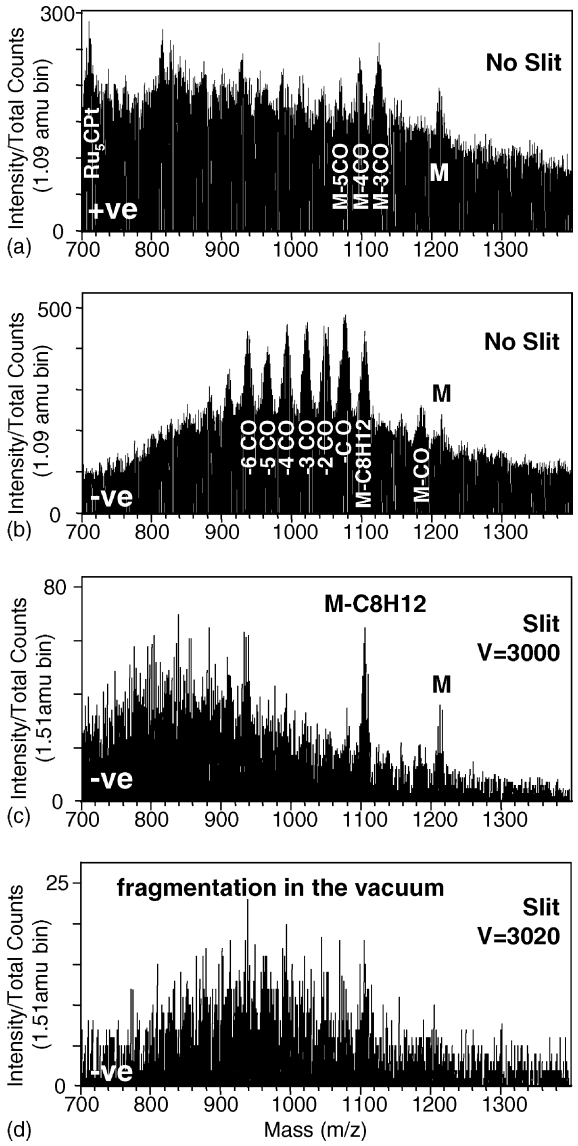

Fig. 2. Partial secondary ion mass spectra of [$Ru_5C(CO)_{14}Pt(C_8H_{12})$] nanoclusters cast on silicon from a solution of acetone: (a) positive mass spectrum in the range 700–1500 Da; (b) negative mass spectrum in the range 700–1500 Da; (c) same as (b), selection of the secondary ions with $\sim 2 \pm 1$ eV of kinetic energy; (d) same as (b), selection of the secondary ions with $\sim 20 \pm 1$ eV of energy deficit with respect to the energy distribution maximum.

ion peaks, due to the Ru and Pt atoms, but also from the presence of an intense background noise covering the whole spectrum. In parallel, the peaks are unusually broad. The use of an energy filter allows us to improve the mass resolution and remove a significant

part of the noise surrounding the molecular ion, thereby demonstrating that they are mostly due to metastable decay reactions after emission, giving rise to series of daughter ions with a kinetic energy deficit [7].

Fig. 2c and d shows the negative mass spectra obtained after inserting a 100 μm energy slit at the crossover following the first electrostatic analyzer. The energy dispersion corresponding to such a slit width is about 1.5 eV. Therefore, it allows us to precisely select ions leaving the surface with a given kinetic energy, or exhibiting a given energy deficit. The mass spectrum of Fig. 2c corresponds to ions having about 2 eV of kinetic energy, i.e. belonging to the maximum of the initial energy distribution. In comparison with the energy-integrated spectrum of Fig. 2b, one notices the almost complete disappearance of the peak series $(M–C_8H_{12}–xCO)^-$, $1 \leq x \leq 5$. The two ions M^- and $(M–C_8H_{12})^-$ remain comparatively intense, indicating that their immediate formation at the sample surface is favored. Note that what appears as a remaining background noise between mass 700 and 1000 Da might be due to cluster fragmentation beyond the energy slit, which should affect the daughter ion trajectories in the rest of the spectrometer, modifying their time-of-flight and, therefore, their position in the spectrum. The mass spectrum of Fig. 2d, corresponding to ions with an energy deficit of 20 eV (i.e. ions having lost a part of their acceleration energy via the loss of a neutral fragment), mostly exhibits background noise, with some features where the molecular fragment $(M–C_8H_{12})^-$ is expected. There is no molecular ion peak, that is, the molecular ion is definitely formed at the sample surface. In this mass spectrum, the intensity is distributed between 800 and 1150 Da, which corresponds roughly to the range of the $(M–C_8H_{12}–xCO)^-$ ion series in Fig. 2b. The fact that these ions series does not clearly emerge from the noise in Fig. 2d is probably due to the energy selection by the slit, which integrates the signal of a 1.5 eV width slab in a distribution of energy deficits extending over a maximum range of 3000 eV (low statistics).

3.2. Comparison with MALDI

Fig. 3 shows the negative MALDI spectrum of $[Ru_5C(CO)_{14}Pt(C_8H_{12})]$ embedded in dithranol. Even

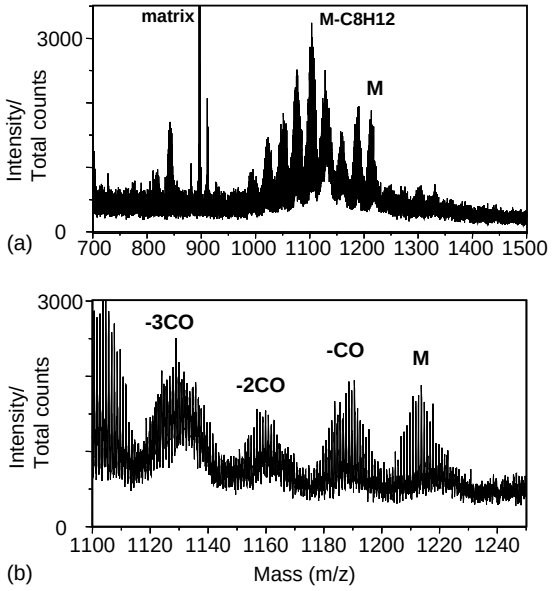

Fig. 3. Negative matrix assisted laser desorption ionization (MALDI) mass spectrum of $[Ru_5C(CO)_{14}Pt(C_8H_{12})]$ nanoclusters embedded in a dithranol matrix: (a) between 700 and 1500 Da; (b) close-up view of the molecular ion region (1100–1250 Da).

though the relative intensities differ, the MALDI spectrum reminds the negative SIMS spectrum displayed in Fig. 2b and the nature of the observed ions is similar, except for some matrix-related peaks (e.g. around 900 Da). The main peaks can be attributed to the molecular ion and to the series $(M–xCO)^-$, $1 \leq x \leq 3$ (4), and $(M–C_8H_{12}–yCO)^-$, $1 \leq y \leq 4$. In the negative SIMS spectrum (Fig. 2b), $(M–C_8H_{12}–yCO)^-$ fragments having lost up to 5–8 CO ligands were also observed, an indication that fragmentation is more extensive under particle bombardment than laser irradiation. As shown in Fig. 3b, the mass resolution of the MALDI spectrum is fairly good and the background noise is significantly less intense in comparison with the SIMS spectrum. The isotopic patterns are well resolved, which was impossible without the use of the energy filter in SIMS.

The peak *broadening* observed in SIMS is the result of very fast decomposition reactions occurring in the acceleration section of the spectrometer, whereas the *background* noise is expected to arise from reactions occurring in this section as well as the rest of the spectrometer. In MALDI, because of the delayed extraction setup (400 ns), a large fraction of these

ions should already be fragmented before entering the acceleration field and, therefore, such reactions should less strongly affect the mass resolution of the instrument. In parallel, one should bear in mind the strongly different optics of the two instruments—triple electrostatic analyzer in SIMS and ion mirror in MALDI—which might have other distinct effects on the measured spectra. Finally, a more fundamental consideration could partly explain the observed differences. Indeed, MALDI is known as a ''soft'' desorption method, because of the specific physics of the laser–surface interaction and the role of the matrix in the energy transfer process. Therefore, the internal energy of the emitted nanoclusters is expected to be lower in MALDI and these clusters should be less prone to fragment in the vacuum. However, this explanation alone is not sufficient, since the MALDI spectra also exhibit intense series of $(M–xCO)^-$ and $(M–C_8H_{12}–yCO)^-$ fragments.

4. Conclusion

The mass spectrometric characterization of molecular Ru–Pt nanoclusters is hampered by the wide isotopic distributions of these elements, but also by the fragility of these large molecular ensembles. The analysis of the ToF-SIMS spectra shows that the molecular ions are mainly produced at the surface whereas the nanoclusters having lost several CO groups, dominant in the mass spectra, are often the result of unimolecular dissociation reactions, both in the acceleration section and the field-free drift tube of the spectrometer. MALDI-ToF provides a similar fragmentation pattern, but with a better mass resolution and a lower background noise. However, embedding the sample in a matrix will be a problem for the direct analysis of supported nanoclusters, which justifies the improvement of ToF-SIMS analysis procedures for this project. The comparison between SIMS and MALDI results suggests, for instance, that either energy filtering or delayed extraction might be very useful for the molecular SIMS analysis of compounds such as these metal nanoclusters bearing fragile residues.

Acknowledgements

AD and SH acknowledge the financial support of the Belgian Fonds National pour la Recherche Scientifique. This work is also supported by the Interuniversity Attraction Pole program on ''Quantum sized effects in nanostructured materials'' of the Belgian Federal State. The ToF-SIMS equipment was acquired with the support of the Région Wallonne and FRFC-Loterie Nationale of Belgium. SH is also grateful to Prof. B.F.G. Johnson (Cambridge, UK) for providing the starting materials for the synthesis.

References

[1] S. Hermans, R. Raja, J.M. Thomas, B.F.G. Johnson, G. Sankar, D. Gleeson, Angew. Chem. Int. Ed. 40 (2001) 1211.
[2] R. Raja, T. Khimyak, J.M. Thomas, S. Hermans, B.F.G. Johnson, Angew. Chem. Int. Ed. 40 (2001) 4638.
[3] B.F.G. Johnson, J.S. McIndoe, Coord. Chem. Rev. 200–202 (2000) 901.
[4] S. Hermans, T. Khimyak, B.F.G. Johnson, J. Chem. Soc., Dalton Trans. (2001) 3295.
[5] B.W. Schueler, Microsc. Microanal. Microstruct. 3 (1992) 119.
[6] A. Delcorte, X. Vanden Eynde, P. Bertrand, D.F. Reich, Int. J. Mass Spectrom. 189 (1999) 133.
[7] A. Delcorte, P. Bertrand, Int. J. Mass Spectrom. 184 (1999) 217.